International Journal of Nanomedicine

Dovepress
Taylor & Francis Group

Open Access Full Text Article

ORIGINAL RESEARCH

Effectiveness of Microwave Therapy Combined with Berberine /GelMA via COX-2/IL-1β Pathway to Treat Skeletal Muscle Injury: An in vivo Study in Rats

Tianhao Du[1–3,*], Liangliang Zhou[1,4,*], Jia Liu[1,*], Xiao Wang[1,2], Haoxu Xie[1,2], Xu Yang[1], Yingxin Yang[1]

[1]Department of Rehabilitation Medicine, General Hospital of Northern Theater Command, Shenyang, People's Republic of China; [2]Liaoning University of traditional Chinese Medicine, Shenyang, People's Republic of China; [3]Hebei Province Hospital of Traditional Chinese Medicine, Shijiazhuang, People's Republic of China; [4]Department of Orthopedics, The Fourth Affiliated Hospital of China Medical University, Shenyang, People's Republic of China

*These authors contributed equally to this work

Correspondence: Yingxin Yang, General Hospital of Northern Theater Command, No. 83, Culture Road, Shenhe District, Shenyang, Liaoning Province, People's Republic of China, Email qjrszx@163.com

Introduction: Skeletal muscle injuries are short-term, that occur in people who play sports and train. Regular exercise and sports populations undergo repetitive tearing and regeneration of skeletal muscle, in which muscle damage is a necessary component to produce an oxidative inflammatory response and tissue reconstruction. The primary goals of treating this illness are to reduce the disease process cycle and get rid of symptoms like swelling and inflammation at the site of localized injury. Berberine (BBR) has several pharmacological effects, including anti-inflammatory, anti-tumor, and anti-arrhythmic properties.

Methods: In order to treat skeletal muscle injuries, a safe and non-toxic nanogel (BBR/GelMA) was developed for efficient berberine delivery. It also investigated whether BBR/GelMA had anti-inflammatory properties via the NF-κB pathway. Microwave irradiation was added to promote the uptake of BBR in BBR/GelMA by injured skeletal muscle and to accelerate the process of injury recovery.

Results: It turns out that the survival rates of NIH313 and L929 cells decreased to varying degrees in GelMA loaded with different concentrations of BBR, but the survival rates of the two cell lines were the highest at a concentration of 0.125 mg/mL.

Conclusion: In this experiment, the inhibitory effect of BBR/GelMA on inflammation was studied. After NIH-313 and L929 cells were treated with GelMA loaded with different doses of BBR, it was found that the concentration of BBR/0.5 mg/mL had the best inhibitory effect on these two inflammation-inducing cell lines, and this inhibitory effect was related to the drug loading concentration. On the other hand, BBR/GelMA and microwave therapy can play an anti-inflammatory and repairing role in skeletal muscle through NF-κB pathway. In addition, microwave can accelerate the diffusion of BBR in BBR/GelMA within injured skeletal muscle, speeding up the healing process after skeletal muscle injury and shortening the disease cycle.

Keywords: skeletal muscle injury, microwave therapy, berberine, GelMA

Introduction

Musculoskeletal problems are rising quickly due to aging and population expansion. Approximately 1.71 billion people are currently affected by musculoskeletal disorders in world.[1,2] Sterile inflammatory and skeletal muscle injury are the most frequent clinical signs of skeletal muscle illness, accompanied by persistent pain, limited mobility and overall function.[3] Sterile inflammatory is a pathological reaction produced by the body without any microbial induction[4,5] Skeletal muscle injury typically sets off a cascade of inflammatory reactions. It is distinguished by the influx of macrophages and neutrophils as well as the generation of pro-inflammatory chemokines and cytokines, including

Received: 2 November 2024
Accepted: 3 April 2025
Published: 28 April 2025

interleukin-1 (IL-1) and tumor necrosis factor (TNF).[6] In addition, T-lymphocytes and other immune cells have a role in muscle inflammation; these cells work with cytokines to control the process of muscle fibrosis and healing.[7] The last stage of inflammation includes angiogenesis, the creation and modification of scar tissue, the regeneration of damaged muscle fibers, and the restoration of muscular function.[8] When it comes to treating skeletal muscle injuries, emergency management—which includes rest, ice, elevation, and compression—should be carried out as soon as possible to maximize the healing muscle's regeneration, return the damaged skeletal muscle to its pre-injury levels of flexibility and strength, and quicken the inflammatory decompensation process.[9]

Currently, in clinical practice, the main goal of treating skeletal muscle injuries is to reduce pain and inhibit inflammation, including both pharmacologic and nonpharmacologic treatments. Pharmacologic treatments include painkillers and anti-inflammatory drugs. Nonpharmacologic treatments include massage, heat, ice, and physical therapy.[10,11] All these therapy choices have the potential to alleviate the symptoms connected to musculoskeletal problems, but they frequently have a variety of unfavorable side effects. In order to reduce the possibility of unfavorable outcomes, it is necessary to develop efficient therapies for alternative and combination treatments for the treatment of musculoskeletal problems. Recent studies have shown that gel patches or creams have excellent pain-relieving and anti-inflammatory effects as commonly used clinically for the treatment of sudden skeletal muscle injuries, so a gel patch was selected for this experiment to treat skeletal muscle injuries in rats (Scheme 1).[12]

In recent times, there has been a surge in study on the topical use of berberine (BBR), a medication used to treat gastrointestinal issues. Berberine, a bitter alkaloid molecule with anti-inflammatory characteristics, has been utilized in the treatment of a range of ailments, including cancer, digestive problems, metabolic disorders, cardiovascular diseases, and musculoskeletal disorders.BBR may potentially slow down the progression of osteoporosis, osteoarthritis, and rheumatoid. Since BBR powder alone does not adhere well to the skin surface when applied topically, a carrier is needed to adhere to the skin surface of rats.[13,14]

Gelatin Methacrylate (GelMA), a photopolymerizable hydrogel made from gelatin, was utilized as a nanomaterial frequently used as a drug substrate in experiments. Gelatin methacrylate has recently gained interest as a material for tissue engineering applications.[14] Because of their excellent biological qualities and predictable physical properties, gelatin methacrylate (GelMA) hydrogels are widely employed in different biomedical applications. These hydrogels closely mirror some of the fundamental features of natural extracellular matrix (ECM).[15] When it comes to musculoskeletal conditions including osteoarthritis, intervertebral disc degeneration, bone and cartilage regeneration, and tendon

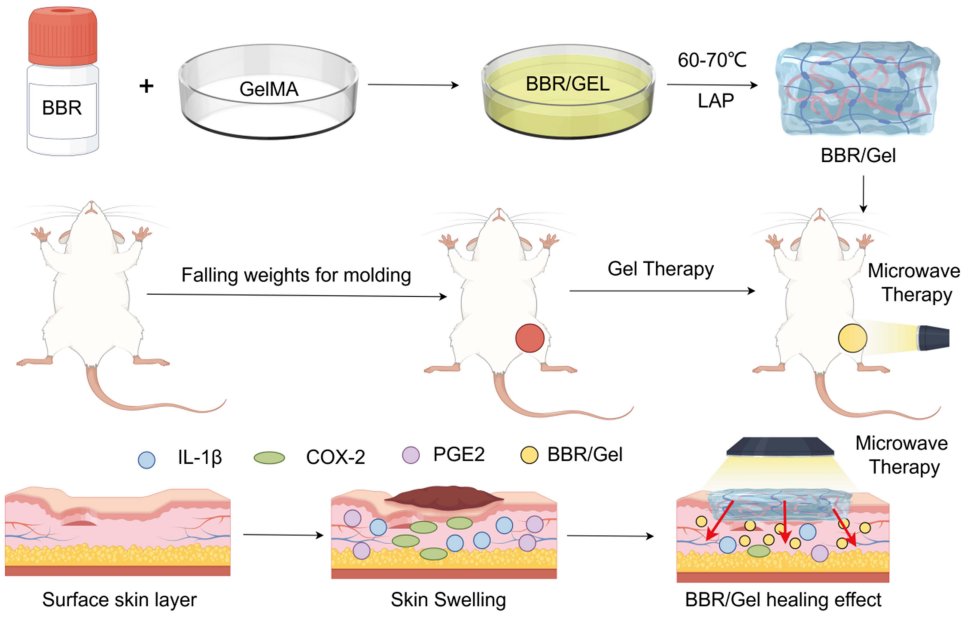

Scheme 1 Schematic diagram of the technical route of this experiment.

problems, GelMA nanocomposites are crucial.[16,17] Recent studies have shown that GelMA, a berberine-containing nanobiomaterial, also has better biocompatibility, good cell survival, proliferation, and cell differentiation responses.[18] Consequently, a composite nanogel of BBR/GelMA was created by adding BBR powder to the GelMA that was already set up for treating skeletal muscle injury in rats.

In the early stages of skeletal muscle injury, the composite nanogel of BBR/GelMA alone is beneficial. However, because BBR absorbs slowly, a "catalyst" must be selected to speed up BBR absorption at the specific injury location. Physical factor therapy is also one of the effective methods for treating skeletal muscle injury, which mainly includes electrotherapy, phototherapy, microwave therapy and heat therapy. Among them, microwave therapy is widely used because of its less side effects. Microwave thermotherapy is through microwave irradiation of local lesion tissues, so that the lesion tissues themselves produce heat, when the heat reaches a certain level, the human body for the changes in the blood supply of the lesion site, improve the local blood circulation, so as to play a role in eliminating inflammation.[19,20] Different frequencies of microwaves have different penetration characteristics and thermogenic power. Since 915MHz microwaves have a low thermogenic power and a deep tissue penetration depth of 10–13 cm, they are employed in the therapy of skeletal muscle injuries. Therefore, 915 MHz microwaves were introduced in this experiment to accelerate the absorption of BBR in the composite nanogel of BBR/GelMA, to achieve a rapid treatment effect of skeletal muscle injury.

Studies have shown that BBR can ameliorate the phenotype of a variety of diseases, particularly by modulating the TLR/NF-kB signaling pathway.[21] It has been shown that BBR can reduce the inflammatory response in macrophages by modifying this signaling pathway (particularly through a SIRT 1-dependent mechanism) to block the inflammatory response.[22,23] In addition, BBR controls inflammatory responses through the protease B and Toll-like receptor 4 signaling pathways (AMPK)[24,25] to control the inflammatory response. In orthopedic diseases, safranin slows the progression of rheumatoid arthritis, osteoporosis, and osteoarthritis.[26] Studies have confirmed that BBR inhibits the release of inflammatory mediators following skeletal muscle injury, and that muscle injury and healing processes are influenced by the TLR 4/NF-kB pathway, which is largely responsible for BBR control of inflammation and macrophages.[27] Thus, using the NF-κB pathway, this investigation also examined the impact of BBR on the expression levels of inflammatory markers in rat skeletal muscle, including interleukin-1β (IL-1β), cyclooxygenase-2 (COX-2), and prostaglandin E2 (PGE2). Investigations were conducted on the impacts and biological processes of various therapy techniques for skeletal muscle injury.

Materials and Methods

Materials

GelMA hydrogel is purchased from Engineering For Life (China). Berberine is purchased from Dalian Meilun Biological Co., LTD (China). SD rats were purchased from Huafukang Biological Company (China). 915 MHz microwave instrument was purchased from Nova Medical Company (China). NIH-3T3 cell was purchased from the American Type Culture Collection (ATCC). LPS was purchased from Solarbio (China). Fetal bovine serum (FBS), penicillin and streptomycin (P/S), Dulbecco's modified eagle medium (DMEM) were procured from Thermo Fisher Scientific (Massachusetts, USA). FreeZol Reagent, M-MLV (H-) Reverse Transcriptase, ChamQ Universal SYBR qPCR Master Mix were purchased from Vazyme (China). IL-1β, COX-2, GAPDH and goat-anti-rabbit antibodies were purchased from Signalway Antibody (USA). PGE2 and IL-1β Elisa kit were purchased from Abmart (China).

Synthesis and Preparation of BBR/GelMA Gels

Take 20 mL of sterile PBS (Biosharp, China), add it into a brown bottle containing 0.05 g of initiator LAP, and dissolve it by heating in a water bath at 50°C for 15 min, during which it was constantly shaken and shaken until LAP was completely dissolved, and then a standard solution of initiator was prepared. Take 1 g of GelMA (Suzhou Yongqin, China) solid into a centrifuge tube, add 20 mL of initiator standard solution, shake to make GelMA fully infiltrated, and place it in a 70°C water bath heated for 30 minutes away from light, during which it was repeatedly shaken until the solid was completely dissolved. BBR (Dalian Meilun, China) was weighed at 1.2 mg/mL, incorporated into the configured GelMA solution, and continued to be dissolved by repeated shaking, followed by immediate filtration through a 0.22 μm sterile needle filter. Coagulation using visible light irradiation at a wavelength of 420 nm. BBR/GelMA hydrogel was

pre-cooled at −80°C for 72 hours. Then the gel was freeze-dried by vacuum freeze-drying machine and the micro-structure of the gel was observed by scanning electron microscope (SEM).

Drug Release Rate

Under aseptic environment, berberine powder with calculated quality was incorporated into the configured GelMA solution and mixed well to obtain berberine GelMA mixture. To properly incubate the gel, the berberine GelMA pre-gel mixture was poured into a 6-well plate (2.5 mL/well) and placed in an incubator set at 37°C. Each well received 2 mL of simulated bodily fluid (SBF) after incubation, and the wells were then kept at 37 °C for additional incubation. 500μL of supernatant was taken from each well after 0.5,1,2,4,8, and 12 hours of incubation, and the same volume of SBF solution was added to each well. Using enzyme markers, the optical density (OD) values of the collected supernatants were determined, and the amount of berberine present in the supernatants at each time point was calculated. The formula for calculating cumulative release rate was as follows: Fi = ∑Ci /(dose * drug content). Plotting the cumulative release curve involves determining the systemic cumulative release (Fi) of the sample and the drug concentration released from the sample (Ci).

Cytotoxicity Assay

The impact of BBR/GelMA on normal cell survival and its suppressive effect on inflammatory cells were assessed using the quantitative CCK-8 cytotoxicity test. To put it briefly, 96-well plates were infected with L929 and NIH-3T3 at a density of 1×104 mL-1. For two-dimensional growth, GelMA loaded with various BBR concentrations (0.0625,0.125,0.25 and 0.5 mg/mL) was then applied. The whole cell medium was then introduced. For two hours, incubate at 37°C with 5% CO2. After that, add 10μL of CCK8 solution and incubate for a further two hours. At 0, 1, 2, 3 and 4 days, the OD value was detected and recorded at 450 nm. As a control, cells grown on fresh media were employed. In addition, NIH-3T3 and L929 cell lines (Purchased from Cell Bank of China Academy of Sciences; GMP standards) by LPS were treated in the same way. Cell viability and inhibition were calculated in treatment group and control group.

Breeding of Experimental Animals

35 male, healthy Specific Pathogen Free (SPF) grade Sprague Dawley (SD) rats (Huafukang Biological Company, Beijing, China; Follow the "3R" principle of the guideline for laboratory animal welfare) weighing between 250 and 300g and seven to eight weeks old were kept in the Animal Experiment Center of China Medical University in a 12-hour light/12-hour light-free environment with two animals per cage, a controlled laboratory temperature of (25±1)°C, and free access to food and water for a week. Water, acclimatization feeding for 1 week. The animals were fasted for 12h before the experiment. This study involving animals was approved by the Animal Ethics Committee of the Northern Theater Command General Hospital (Approval No. 2023-16, Ethics Date:2023-4-20). All animal husbandry and experiments were conducted in strict accordance with the management and use regulations for laboratory animals.

Grouping of Experimental Animals

Using the random number table method, the 35 SD rats were numbered and split into 5 groups of 7 animals each: The NC group was a blank group with no modeling or treatment, the Model group was only treated muscle injury, the Mi group was only microwave treatment, the BBR/Gel group was treatment with berberine GelMA, and the Mi+BBR/Gel group was treated by berberine GELMA combined with microwave. The model was assessed after modelling and then the groups received microwave and drug treatments according to the appropriate intervention plan.

915HMz Microwave Therapy Mode and BBR/GelMA Gel Delivery Mode

Referring to the relevant literature to determine the appropriate biotherapeutic microwave energy (915MHz microwave therapy instrument), the intermediate value was used, and the irradiation was carried out for 10 minutes at 10W energy intensity and 10cm treatment height.[28] The microwave group and BBR/Gel combined microwave group were given 10 minutes of microwave therapy daily for 1 week. BBR/Gel and BBR/Gel combined microwave group rats were coated with BBR-loaded gel on the affected epidermis and continued to be coated every other day for 7 days.

Construction of Muscle Injury Model

Surgical modeling of each SD rats expect NC group was carried out by the free-fall method.[29] Before the experiment, each SD rat was weighed and recorded, and then anesthetized by inhalation with isoflurane, a gas inhalation anesthesia machine. Following anesthesia, the rats were strapped to the operating table in a supine position, and animal hair removal lotion was used to depilate the skin of the right calf and gastrocnemius muscle. The modeling site was marked, and the position of plastic tube was determined. A plastic tube of about 60 cm in length and 6cm in diameter was placed vertically on the marked site, and the modeling site was hit by a 200 g weight in the free-fall, and the process was repeated 6 times. When there are local red spots, swelling, bruising and no epidermal damage or fracture dislocation, etc., it is regarded as successful modeling.

Rate of Calf Muscle Swelling

Measure the circumference of the central part of the rat's calf muscle injury before modeling, record the data, and then measure the circumference of the central part of the rat's calf muscle injury 1 hour after the end of the modeling, and calculate the muscle swelling rate (MSR) with the formula MSR=(S/S0-1)×100%, in which S0 is the circumference of the central part of the rat's calf muscle injury before the modeling, and S is the circumference of the central part of the rat's calf muscle injury 1 hour after the modeling. S is the circumference of the center of calf muscle injury 1 hour after modeling.[30]

Assessment of Injury Symptom Index

After molding, the molding limbs were scored according to the following criteria and re-evaluated on the 7th day.[31]

(1) Degree of bruising: dark purple 2 points, dark red 1 point, normal color 0 points;
(2) Degree of swelling: obvious swelling 2 points, slightly swollen 1 point, no swelling 0 points;
(3) Degree of mobility: the modeled limb can not be acted on 2 points, poor mobility of the modeled limb 1 point, normal mobility of the modeled limb 0 points.

Footprint Experiment

Each group were feed in a suitable environment for 1 day after modeling, and the tracks were collected on 1, 4, 7 day. We used a 50 cm* 6 cm* 7 cm cuboid runway and placed a 50 cm*6 cm paper inside it.[32] Before the footprints were collected, the rat was placed in front of the runway to acclimate. Then the feet of rat were dipped in ink and placed on the runway. When the rat reached the end of the race, the paper was removed. The stride width, stride length and stride pitch were measured and recorded.

Serum and Specimen Collection

1 mL of fresh blood was extracted from the inner canthus of each rat group's eye on days 1, 4, and 7 following successful modeling. The blood was centrifuged at 3500 rpm for 15 minutes, and the supernatant was extracted. The serum was stored at −80°C and used for Elisa assay. SD rats were executed by carbon dioxide asphyxiation. 50–100mg of tissue at the center of right leg muscle injury was clipped from each group and stored in a low-temperature refrigerator (−80°C) for WB detection and PCR assay. The tissue was then sliced, clipped, and fixed in 4% paraformaldehyde solution for HE staining and immunohistochemical examination, measuring 1.0 cm by 1.0 cm by 0.5 cm.

RT-qPCR

After 7 days, the expression of the genes related to inflammation was assessed using real-time quantitative polymerase chain reaction (qPCR). To put it briefly, FreeZol Reagent (Vazyme, Nanjing, China) was used to separate the total RNA from isolated muscle tissue of a calf. Next, M-MLV (H-) Reverse Transcriptase (Vazyme, Nanjing, China) converted RNA to cDNA. ChamQ Universal SYBR qPCR Master Mix (Vazyme, Nanjing, China) was used for the QPCR process. Thermo Fisher Scientific, USA's QuantStudio real-time fluorescence quantitative PCR equipment was used to perform RT-PCR in order to assess the expression of the inflammatory genes COX-22 and IL-1β. The reference gene was glyceraldehyde 3-phosphate dehydrogenase (GAPDH). The $2^{-\Delta\Delta CT}$ technique was used to calculate the relative gene expression. Table 1 provided the primer sequences for GAPDH, COX-2, and IL-1β.

Table 1 Reverse Transcription Primer Sequence

Primer Name	Primer Sequence
GAPDH-F	GACATGCCGCCTGGAGAAAC
GAPDH-R	AGCCCAGGATGCCCTTTAGT
IL-1β-F	CTTCAAATCTCACAGCAGCAT
IL-1β-R	CAGGTCGTCATCATCCCAC
COX-2-F	CACGGACTTGCTCACTTTG
COX-2-R	AGCGTTTGCGGTACTCATT

Western Blotting (WB)

Using a complete protein extraction kit (Solarbio life science, Beijing, China), the protein from the muscle tissue was isolated. The protein was measured by using the BCA kit (Biosharp, Anhui, China) and was denatured using 5* loading buffer (Biosharp, Anhui, China). After electrophoresis, transmodeling, containment, and TBST solution cleaning treatment, incubate with primary antibodies overnight. Primary antibodies included IL-1β, COX-2 and GAPDH (Signalway Antibody, USA). After one hour of heating with goat anti-rabbit antibody (Signalway Antibody, USA), the membranes were finally cleaned with TBST solution. Tanon, Shanghai, China's high-sig ECL Western blotting substrate was used to see the protein bands. Using IMAGE J software, each band's gray scale value was found, and the relative expression levels of the proteins in each sample were computed.

Enzyme-Linked Immunosorbent Assay (ELISA)

We used PGE2 and IL-1β Elisa kit (Abmart, Shanghai, China) to detect secretion levels. According to the instructions of the enzyme immunoassay kit, the experiment was carried out according to the following steps: the collected rat serum drops were added to the micropore plate provided by the kit, incubated at 37°C for 30 minutes, then washed and added with enzyme-labeled reagent, incubated again for 30 minutes, washed and added with chromogenic solution for color development. The corresponding OD values were detected under the enzyme-labeled instrument, and the standard curve was drawn to calculate the expression level of PGE2 and IL-1β.

H&E Staining

The following protocol was used to deparaffinize the prepared sections: two times (5 min/time) in xylene, deparaffinization - five minutes of anhydrous ethanol dehydration - two minutes of 95% ethanol hydration - two minutes of 80% ethanol hydration - two minutes of 70% ethanol hydration - Hydration with diluted water for two minutes - Staining with hematoxylin for five to ten minutes - A 30-second differentiation solution - The treatment protocol involved immersing in tap water for 15 minutes, rinsing with tap water after 2 minutes, and then immersing in tap water again for 4 minutes, culminating in dehydration. For two minutes, each of the following ethanol concentrations will be used: 50%, 70%, 95%, 100%, and 100%; for two minutes, 1× and 2× xylene will be cleared; the slices will then be sealed with neutral resin to keep the film sealed examined under a microscope and captured on camera.

Immunohistochemistry (IHC)

Following their dewaxed and hydrated state, the prepared sections were permeabilized for half an hour at room temperature using the closed permeabilization solution, and then placed out of direct sunlight. They were then cleaned thereafter. After immersing the pieces in a 0.01 M sodium citrate buffer solution (pH = 6.0), they were heated. After that, clean the box with PBS solution, take out the sections, and add 5% goat serum. Next, warm the primary and secondary antibodies, add SP, and bake it for 30 minutes at 37°C. Finally, wash the box with PBS, add DAB (fast drop), watch the staining, and adjust the time it takes for the color to develop. Washing with PBS with double-distilled water; add large drops of hematoxylin staining solution to stain cytoplasmic proteins and cytoplasmic or cytoplasmic membrane proteins. Then rinse with tap water, wash with double-distilled water, and then restore the blue color with PBS for 5 minutes. The portions were then sealed with neutral gum and dried examined under a microscope and captured on camera.

Statistical Analysis

In this study, statistical analysis tools SPSS 26.0 and GraphPad Prism 8 were used to evaluate the data. All data are presented in the form of mean ± standard deviation (SD) for easy understanding and comparison. All the results of this experiment used One-way ANOVA as the main statistical method, such as WB, RT- qPCR and Elisa. Prior to ANOVA analysis, we first performed a normality test on the data, using the Shapiro–Wilk test to assess whether the sample conforms to a normal distribution. At the same time, Bartlett test was also conducted to evaluate the variance homogeneity of each group of data. These two tests ensure that ANOVA's preconditions are met. Once we confirm that the data satisfy normality and homogeneity of variance, we perform ANOVA analysis. The ANOVA results used P-values to determine the significance of the differences between groups. Specifically, when $p > 0.05$, we considered that the difference between the groups was not statistically significant; When $p < 0.05$, there was a statistically significant difference between the groups. In addition, to further explore the specific sources of differences between groups, when ANOVA results were significant, we used post-hoc tests, such as Tukey's HSD test, to compare specific differences between groups and identify which groups had significant differences. Bilateral tests were used for all statistical analyses, and the statistical significance level was set at $\alpha = 0.05$. The above statistical methods ensure the reliability and scientificity of the results.

Results

Synthesis and Characterization of BBR/GelMA Hydrogels

As seen in Figure 1A, photoinitiator LAP may be used to photocrosslink the synthesized GelMA and BBR when exposed to UV light. The hydrogels were shown to be porous by scanning electron microscopy (SEM) findings, and Figure 1B illustrates the scaffold's ordered porosity structure. Furthermore, the inclusion of BBR causes the gel's pore size to shrink and its density to increase, allowing normal cells to adhere to it and proliferate.[29] The chemical structures of BBR and GelMA revealed that the composite hydrogels had a large amount of hydrogen and ionic bonds created by hydroxyl, carboxyl, amine, and sulfonic acid groups, as well as amide and C-C covalent bonds produced by the reaction of carbodiimide and free radicals, respectively (Figure 1C).

When skeletal muscle is normally injured, inflammatory cells release large amounts of inflammatory factors, which cause apoptosis in some skeletal muscle cells. However, when the injury is prolonged, uncontrollable inflammatory cells (mainly neutrophils and macrophages) secrete excessive cytokines, exacerbating the inflammatory response and creating a vicious cycle of chronic inflammation. As shown in Figure 2A and B, the survival rate of NIH313 and L929 cells decreased to different degrees in GelMA loaded with different concentrations of BBR, but the rate was the highest at the concentration of 0.125mg/mL in both cell lines. NIH-313 and L929 cells were treated with GelMA loaded with varying doses of BBR in order to create an inflammatory model and examine the inhibitory impact of BBR/GelMA on inflammation. The findings demonstrated that after two days, four different concentrations of BBR/GelMA had a strong antibacterial effect. On the two inflammation-induced cell lines, the best inhibitory effect was achieved by the BBR/0.5 mg/mL concentration, and this inhibitory effect was correlated with the drug loading concentration (Figure 2C and D). In summary, 0.125mg/mL concentration of BBR will be used for subsequent cell experiments.In addition, according to the IC50 value of BBR/Gel on cells (Figure 2E) and dose-response curve (Figure 2F), a 1.2 mg/mL concentration of BBR/GelMA was used to treat the soft tissue damage model in the following experiments.

Effectiveness and Assessment of Skeletal Muscle Injury Modeling

The SD rats were modeled by using the free fall method and treated with a 915MHZ microwave instrument, which was maintained at a height of 10cm. (Figure 3A–D) The movement footprints of the rats were collected on 1, 4, and 7 days (Figure 3E), and the stride length, stride width, and stride pitch were analyzed (Figure 3F–H). The step width of the rats in each group did not substantially vary ($p > 0.05$) at any time point; however, over the course of the next two days, the step width of the Mi+BBR/Gel group fell more dramatically ($p < 0.05$). (Figure 3F) The step widths of the rats in each group were different in Figure 3G at different times, particularly on day 1. The model group's stride pitches were shorter than Mi group's ($p < 0.05$), and on day 4, the stride pitches of the Mi+BBR/Gel group were significantly shorter ($p < 0.05$) than the BBR/Gel group's. After analyzing the step size change in each group, it was discovered that the Mi group and the Mi+BBR/Gel group saw the biggest decreases in step size, particularly in the Mi+BBR/Gel group shown in

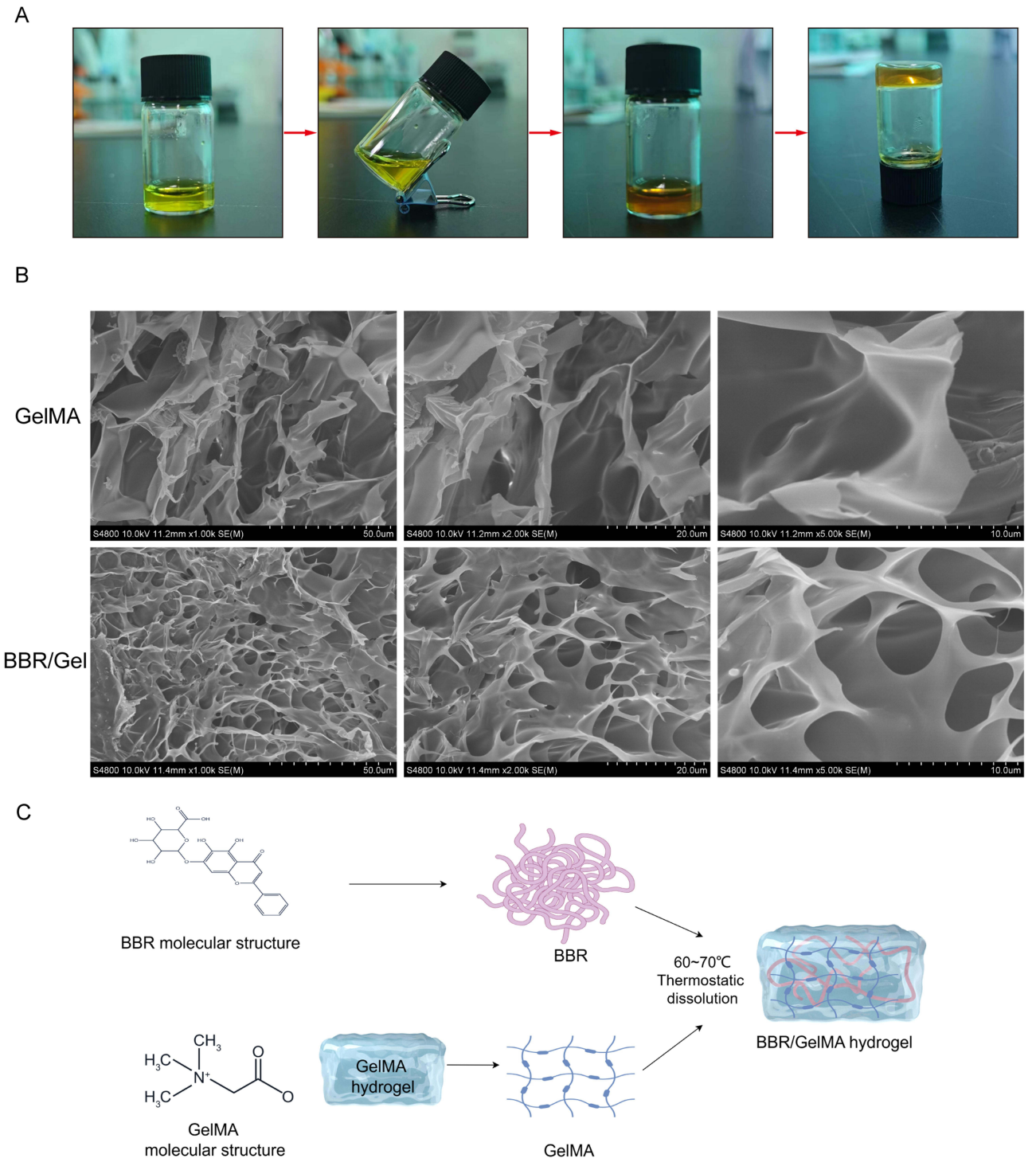

Figure 1 (**A**) Image of BBR/GelMA mixed solution converted to hydrogel after irradiation with light at a wavelength of 420 nm for 30 seconds. (**B**) Scanning electron microscope images and porous structures of GelMA and BBR/GelMA hydrogels. (**C**) Molecular structural formulae of BBR and GelMA and schematic diagram of the binding process.

Figure 3H. In the Mi+BBR/Gel group, there was a substantial reduction between the 1 and 4 days, but no significant change between the 4 and 7 days. After 7 days, compared to model group, the Mi group had shorter stride length, the difference had statistically significant.($p < 0.05$) After analyzing the step length change for three days in each group, we found the Mi +BBR/Gel group reached almost normal on day four. The Mi+BBR/Gel group was significantly shorter

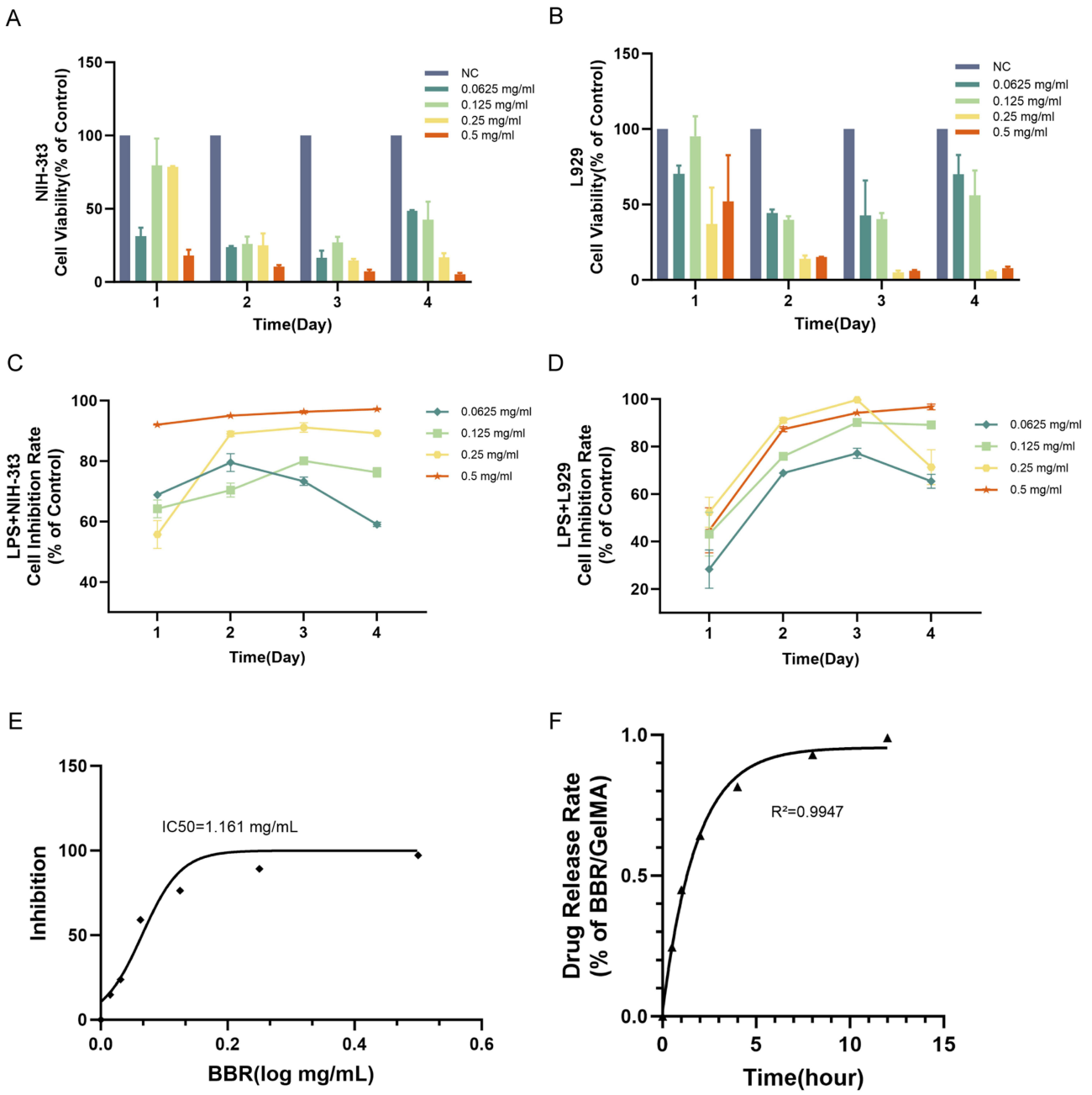

Figure 2 (**A**) Survival of NIH-313 cells at different BBR concentrations (0.0625,0.125,0.25,0.5 mg/mL) over time. (**B**) Survival of L929 cells under different BBR concentrations (0.0625,0.125,0.25,0.5 mg/mL) over time. (**C** and **D**) Inflammatory inhibitory effects of different concentrations of BBR on NIH-313 and L929 cells under LPS induction. (**E**) The optimal concentration of BBR in GelMA, ie IC50 curve. (**F**) Drug release rate of BBR in GelMA over time.

than Model group ($p < 0.05$), but there was no significant difference ($p > 0.05$) with the other groups. Although the stride length was slightly higher in the BBR/Gel group, the difference was not statistically significant. ($p > 0.05$).This process shows that microwave therapy can accelerate the whole process of inflammation occurrence.

The rate of muscle swelling was assessed in each group both before to and following modeling. The outcome demonstrates that there was no significant difference between the model group and the treatment group ($p > 0.05$), indicating that the model is stable (Figure 3I).

Injury index scores were used to assess injury in each group and were recorded on 1 and 7 day. Within a day, the damage index values in the other groups were statistically significant ($p < 0.05$) in comparison to the NC group, demonstrating the

https://doi.org/10.2147/IJN.S500490

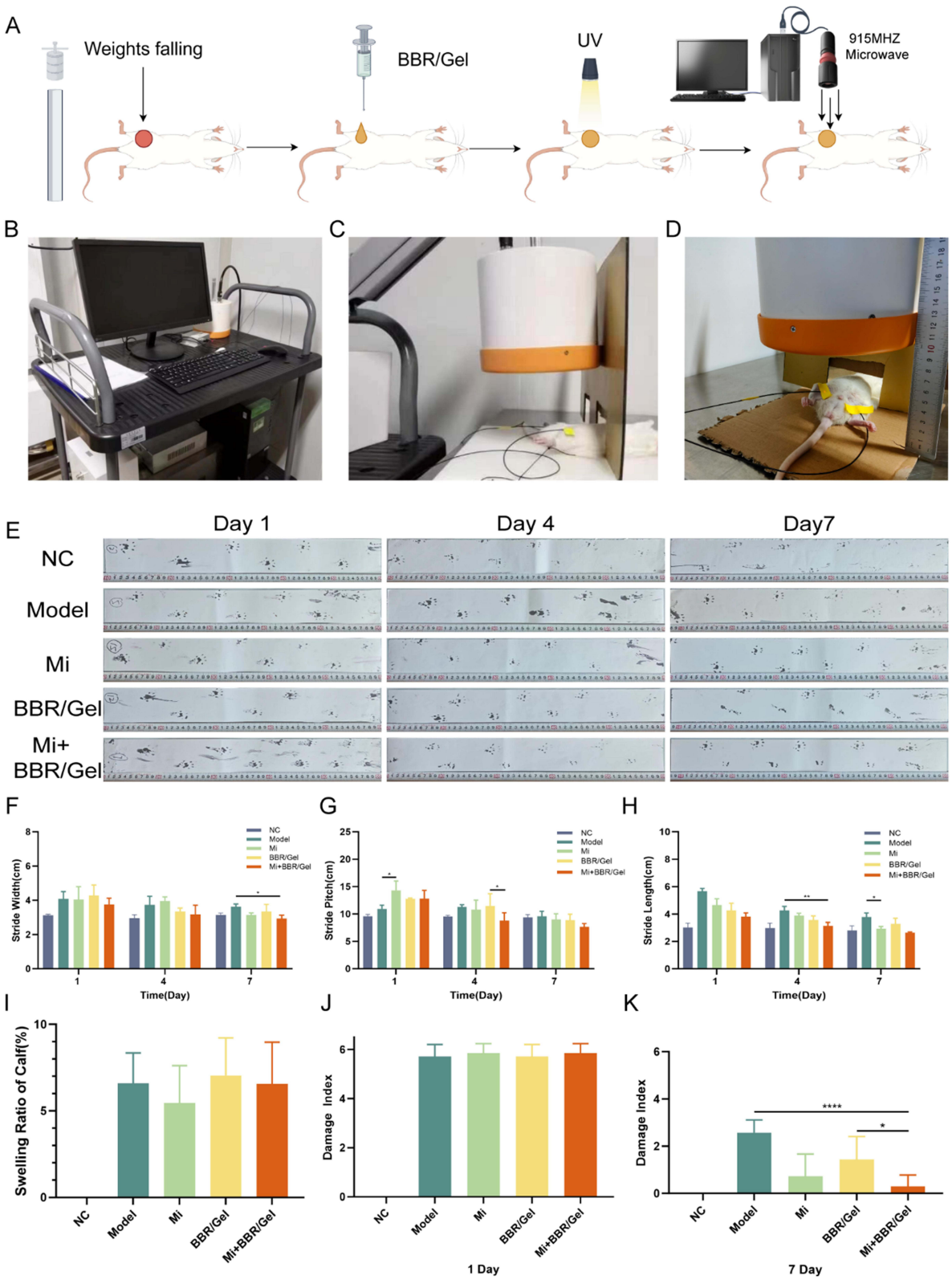

Figure 3 (**A**) Schematic diagram of the process of 915 MHz microwave treatment of Skeletal muscle injury. (**B**) 915 MHz microwave therapeutic instrument. (**C** and **D**) are the effect graphs of the rats that received 915 MHz microwave treatment (shown in high degree). (**E**) the locomotor footprints of the SD rats on 1,4 and 7 days after modeling. (**F**–**H**) the analysis of stride length, stride width and stride pitch of SD rats. (**I**–**K**) the analysis graphs of the calf swelling rate and the damage index after modeling. (*P < 0.05; **P < 0.01; ****P < 0.0001).

stability of the models. (Figure 3J) It's interesting to note that the index of Mi+BBR/GelMA group was lower than Model group, ($p < 0.01$) and the index of Mi+BBR/GelMA was significantly lower than BBR/GelMA group ($p < 0.05$). (Figure 3K)

BBR Combined with Microwave Affects RNA Expression Levels of IL-1β and COX-2 in Skeletal Muscle Injury

Reverse transcription primers were designed, as shown in Table 1, and RT-qPCR experiments were performed. The findings demonstrated that all treatment groups had lower expression levels than the model group, with a statistically significant difference. Notably, the Mi+BBR/Gel group had the lowest expression level ($p < 0.05$). The treatment group and the NC group did not, however, differ significantly ($p > 0.05$). It's interesting to note that the Mi+BBR/Gel group's COX-2 expression level was lower than the NC group's, although the difference was not statistically significant ($p > 0.05$). (Figure 4A and B)

The Effects of BBR and Microwave on Skeletal Muscle Injury Serum IL-1β and PGE2 Expression Levels

Elisa was utilized to measure serum 1.4 and 7 days after modeling in order to investigate the expression levels of PGE2 and IL-1β. The findings demonstrated that all groups' levels of PGE2 and IL-1β expression in SD rats were considerably higher than those of the NC group. All treatment groups showed a reduction in expression levels as compared to the model group. It's interesting to note that the Mi group's protein expression trended upward from the first day, whereas the BBR/Gel group's protein expression level gradually declined. On day 1, the expression levels of the other treatment groups were statistically significantly ($p < 0.05$) lower than those of the Mi group. Although the expression levels of IL-1β and PGE2 in the BBR/Gel group were lower, the difference was not statistically significant with others ($p > 0.05$) on day 4. But the expression levels in the Mi+BBR/Gel group were significantly lower ($p < 0.05$) than other group, expect NC group. Remarkably, by day 7, there was no statistically significant difference ($p > 0.05$) between the Mi group and the Mi+BBR/Gel group. The Mi+BBR/Gel group had lower IL-1β expression levels than the BBR/Gel group, although the difference was only statistically significant on day 7 ($p < 0.05$). The Mi+BBR/Gel group had decreased PGE2 expression levels on days 1 and 4, and this difference was statistically significant ($p < 0.05$) (Figures 4C and D).

BBR Combined with Microwave Affects IL-1β, COX-2 Protein Expression Level in Skeletal Muscle Injury

Western blotting was used to determine the expression levels of COX-2 and IL-1β in the damaged center tissues of each group after seven days. The findings demonstrated that, with the exception of the Mi+BBR/Gel group, the protein expression levels of the other groups had increased to varying degrees as compared to the NC group. The Mi+BBR/Gel group's protein expression level was significantly ($p < 0.05$) lower than that of the model group. In addition, among the treatment groups, Mi+BBR/Gel group produced the best effect, and there was no statistical difference between the Mi +BBR/Gel group and the NC group ($p < 0.05$), and the expression level of the BBR/GeL group was statistically significant. It's interesting to note that while the Mi+BBR/Gel group's protein level was lower than the Mi group's, there was no statistically significant difference between the two groups ($p > 0.05$). Nevertheless, the Mi group's IL-1β expression level differed considerably from the NC group's ($p < 0.05$) (Figure 4E).

Comparison of HE Staining Morphology of Soft Tissue Injury Specimens of Male SD Rats in Various Groups

Figure 5A depicts the postoperative recovery of the rats in each group. Each group's muscle samples were stained with HE to examine the clinical symptoms. The findings demonstrated that there were no aberrant modifications, that the skeletal muscle cells' size distribution was uniform, that the nucleus size was modest, and that the muscle fibers in the NC group were intact. In the model group, skeletal muscle fibers were widely broken, skeletal muscle cell structure was disordered, the hierarchy was unclear, skeletal muscle cells were swollen, enlarged or even died, showed aggregation, nuclear atrophy, and cell structure was incomplete. Myocytes in each treatment group had different degrees of injury,

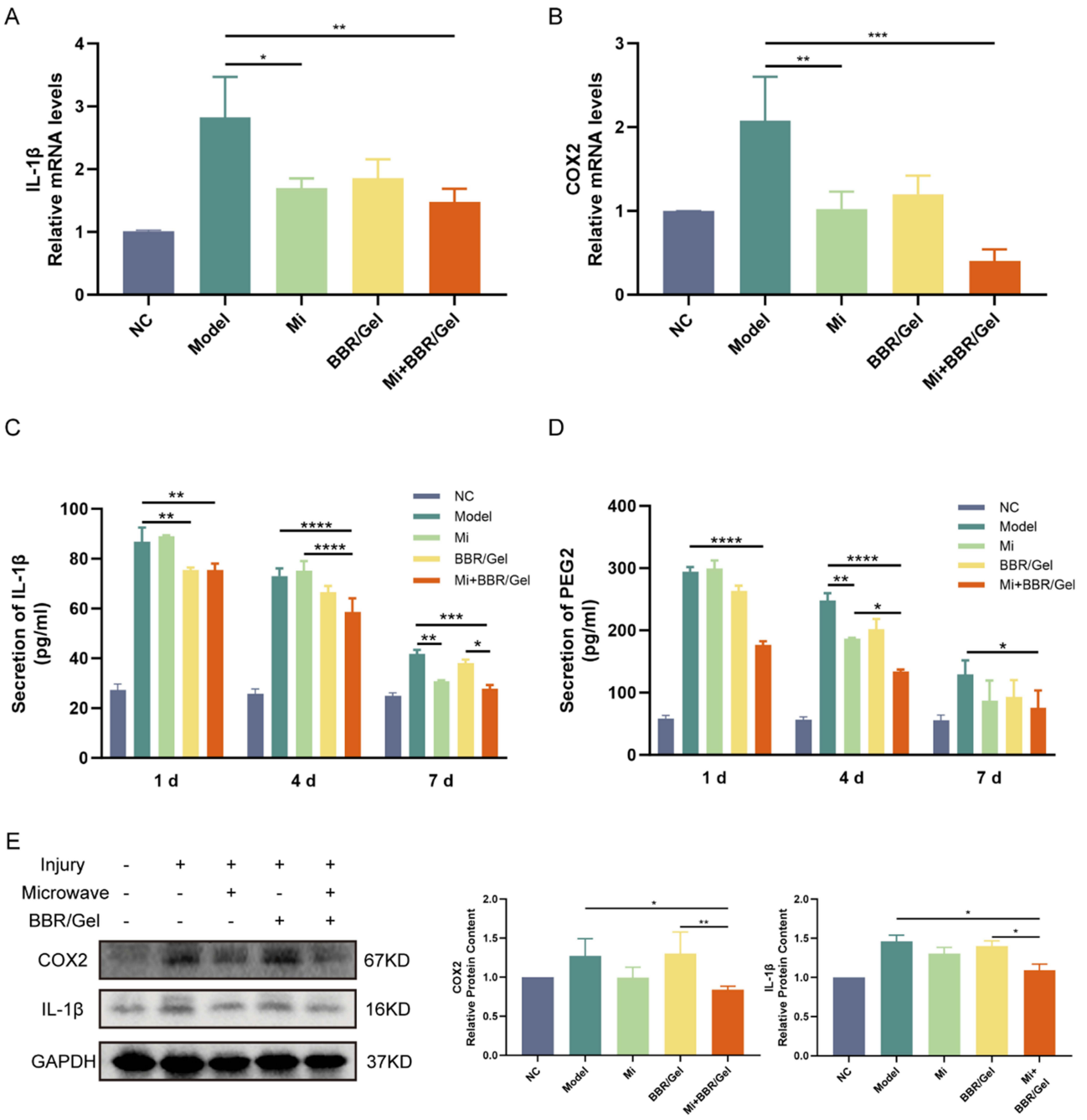

Figure 4 (**A** and **B**) Expression levels of mRNA for IL-1β, COX-2 in skeletal muscle of SD rats in each group. (**C** and **D**) The expression levels of IL-1β, PGE2 in the serum of SD rats in each group at 1/4/7 days after modeling. (**E**) Expression levels of IL-1β, COX-2 in skeletal muscle of SD rats in each group. (*P < 0.05; **P < 0.01; ***P < 0.001; ****P < 0.0001).

myofibrillar tissue disorder, thinning or fracture, inflammatory infiltration of myofibrillar interstroma, mild degeneration and nuclear wrinkling. Under a ×400 lens, the Mi group's degree of skeletal muscle injury was comparable to that of the BBR/Gel group. In line with the outcomes of the WB trial, the Mi+BBR/Gel group had the least amount of skeletal muscle injury (Figure 5B).

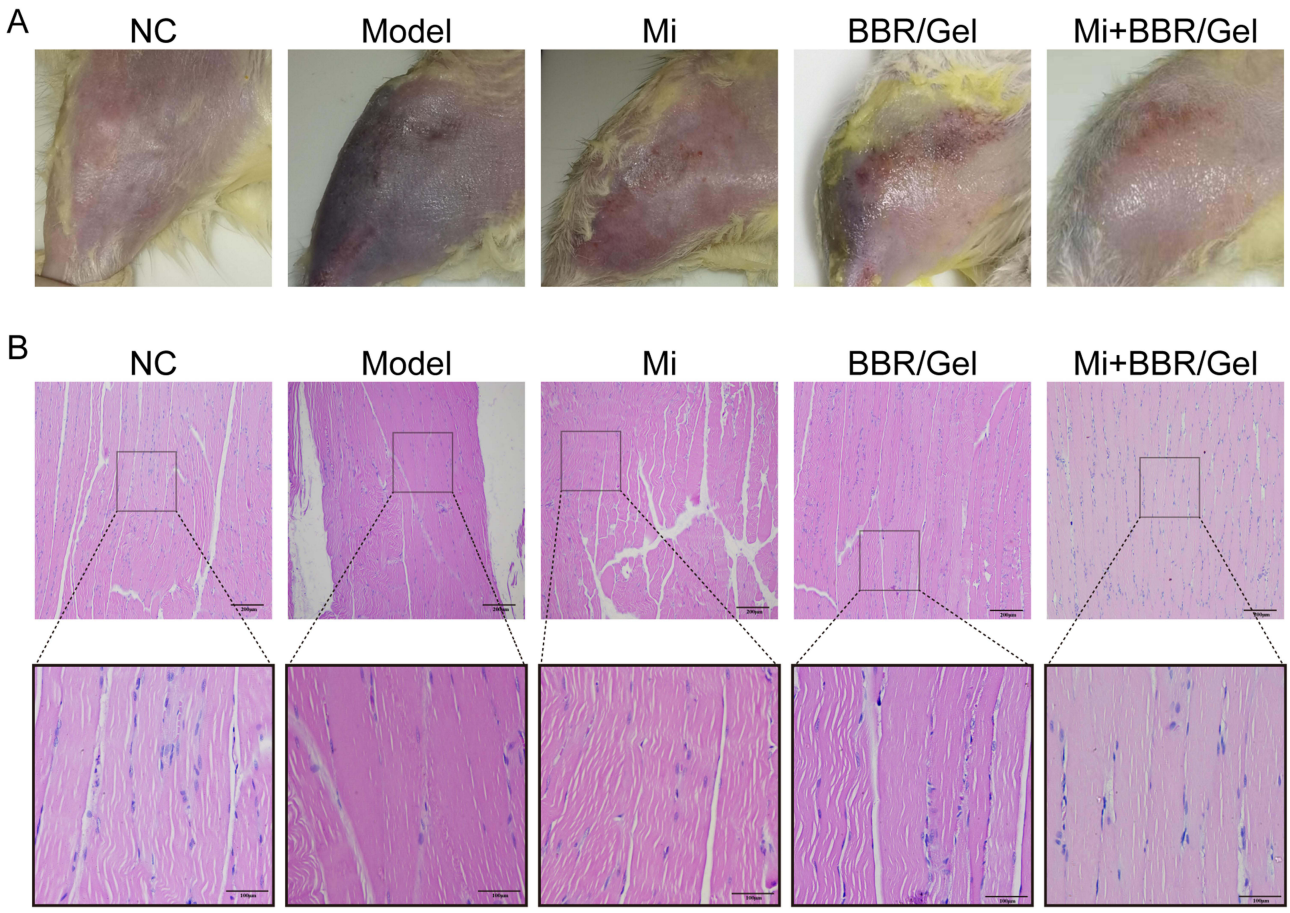

Figure 5 (**A**) Demonstration of modeling effects of soft tissue injury in different groups of SD rats (**B**) Comparison of light microscopy under HE staining of soft tissue damaged tissues in various groups of SD rats. (×100, ×400).

Comparison of Immunohistochemistry Morphology of Soft Tissue Injury Specimens from Groups of Male SD Rats

Immunohistochemistry (IHC) was done on the tissues from each group to determine the expression of COX-2 and IL-1β, and MOD was computed. Figures 6A and B illustrate the levels of IL-1β and COX-2 in the skeletal muscle tissues of the NC group. The contents of these molecules in the model group are significantly higher than those in the NC group, whereas the Mi+BBR/Gel group has the lowest levels of these molecules, but they are still higher than those in the NC group. The contents of two inflammatory variables were not significantly different between the Mi group and the BBR/Gel group, as Figures 6C and D demonstrated, but they were greater in the Mi+BBR/Gel group, with statistical significance ($p < 0.05$). The most effective treatment group appears to be the combination group, and IL-1β and COX-2 subregulation control BBR's impact on the NF-κB pathway.

Discussion

Musculoskeletal impairments are characterized by impairments in the muscles, bones, joints and adjacent connective tissues leading to temporary or lifelong limitations in functioning and participation. Musculoskeletal disorders are typically characterized by pain (usually persistent) as well as limitations in mobility, dexterity and general functioning, and reduced work capacity.[33] Skeletal muscle injury typically sets off a chain reaction of inflammation. Inflammatory cytokines are released by neutrophils and macrophages when they phagocytose tissue debris.[34] These cytokines then encourage myofibroblast fusion and vascularization, which aids in the healing of injured muscle. However, the high degree of immune cell activation and mobilization brought on by the massive release of chemokines and inflammatory

https://doi.org/10.2147/IJN.S500490

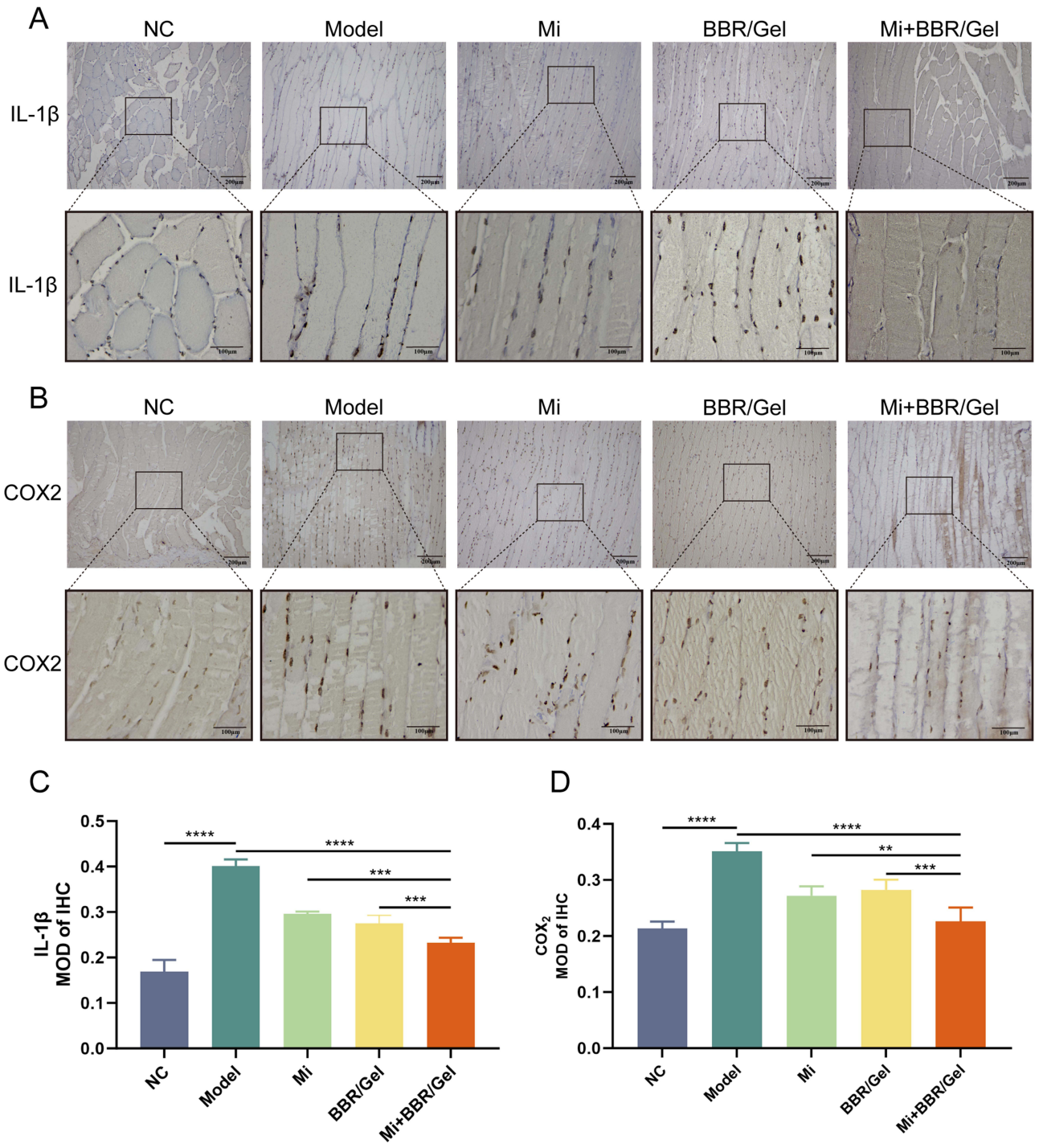

Figure 6 (**A** and **B**) shows the demonstration of IL-1β with COX-2 in immunohistochemical chromogenic results of different groups of SD rats under light microscope. (**C** and **D**) show the correlation analysis of IL-1β with COX-2 in the immunohistochemical color development results of rats. (**P < 0.01; ***P < 0.001; ****P < 0.0001).

substances sets off a vicious cycle that culminates in a cytokine storm. In order to lessen tissue damage, including to healthy bystander tissue, the cytokine storm causes increased amounts of lytic and cytotoxic molecules as well as reactive oxygen species (ROS) in the injured muscle.[35]

The damaged muscle has an inherent potential to repair and heal itself,[36] When elements originating from injured myofibers activate satellite stem cells.[37,38] After proliferating and differentiating, activated satellite stem cells attach to damaged fibers and merge with them to restore their functionality. Simultaneously, immune cells release a lot of

cytokines, such TNF-α, IL-1β, and interleukin 6 (IL-6), which can encourage muscle stem cell growth and repair.[39] However, following tissue damage, infiltrating macrophages use phagocytosis to engulf and digest dead cells and cellular debris. This shifts the macrophage phenotype into healing macrophages, which control angiogenesis, inflammation, myofibroblast fusion growth, fibrosis, and ultimately restore homeostasis.[40,41]

Berberine can reduce the course of osteoporosis, osteoarthritis and rheumatoid arthritis. Berberine's advantageous characteristics are partly attributed to its capacity to selectively target various signaling pathways, such as NF-κB, MAPK, and others. In addition, berberine contains anti-apoptotic, anti-inflammatory and immunosuppressive effects.[34,42] Many studies have been conducted on the mechanism by which BBR regulates pro-inflammatory cytokines. In the Wang et al experiment,[43] PI3K/AKT-related proteins and inflammatory factors were identified using qPCR and WB methods in each group. The findings indicated that the BBR-loaded temperature-sensitive hydrogel group had lower levels, indicating that the hydrogel had an anti-inflammatory impact. BBR has been shown to block the NF-κB inflammatory pathway through the regulation of COX-2, IL-1β, and related molecules including PGE2.[34]

Adipose mesenchymal stem cells were infused into GelMA in the tests conducted by Li et al,[17] the results indicated that hypo-CM-loaded GelMA was more successful in inducing angiogenesis to hasten the repair of skin aging lesions. It was most likely connected to the increased VEGF content, and the mechanism might be as follows. When VEGF is present in hypo-CM, it stimulates the Akt/mTOR and MAPK signaling pathways, which in turn stimulate biological processes like endothelial cell migration and proliferation. This improves blood flow to the injured area and, in the end, aids in wound healing. In wound healing applications, loading reduced graphene oxide (rGO) on GelMA can stimulate angiogenesis, migration, and proliferation of cells.[21]

As a form of physical therapy, microwave therapy cures diseases by utilizing biological and thermal effects. The organism responds most immediately to microwave thermotherapy by raising the temperature of nearby tissues and muscles, and the primary physiological reaction to heat is an increase in local blood flow. On a microscopic level, it is the regulation of cellular and molecular mechanisms. Localized heating increases nutrients and oxygen in the heated area, which are essential for tissue repair. Furthermore, microwave thermotherapy promotes cell membrane permeability, which enhances cytosolic extravasation and makes it possible for granulocytes and macrophages to reach the wounded region.[44] It's interesting to note that heat enhances muscle contractile function by changing the mechanical characteristics of collagen and raising ATPase activity.[45]

Energy-intensive oxidative stress causes inflammatory cells to become activated, move into the wounded muscle, phagocytose necrotic tissues, and produce chemokines and free radicals.[46] Lipid peroxidation is one way that free radicals can harm the structure of muscles and tendons. They can also change proteins and DNA. In rat skeletal muscle, HSPs offer biochemical and ultrastructural defense against ischemia injury, and localized heating can reduce the damage that free radicals do to the muscle.[47] Excessive centrifugal exercise of skeletal muscle induces an increase in intramuscular factors and neutrophils, which have both proinflammatory and anti-inflammatory properties in muscle. It has been demonstrated that muscle factors, including interleukin 6 (IL-6), interleukin 8 (IL-8), and interleukin 15 (IL-15), are related to inflammation and recovery.[48]

Elevated body heat shock protein levels might be linked to the mechanism of action of microwave thermotherapy. One of a group of highly conserved emergency proteins called heat shock proteins (HSP) reacts to a range of physiological and environmental stressors, including as heat, cold, ischemia, hypoxia, and energy deprivation, and helps shield cells from harm.[49] In human skeletal muscle, microwave hyperthermia therapy (MHT) raises the levels of HSP90, HSP72, and HSP27.[50,51] It is well known that muscle overloading can consistently increase muscle mass. Both overloading of muscles and heat stress treatment of muscles can increase the increase of HSP25 and HSP72 in skeletal muscles, but the HSP content of heat stress-treated muscles is much higher than that after overloading exercise.[52] The flounder muscle of mice receiving heat treatment had noticeably elevated levels of HSP70 and HSP25. Several studies have revealed the effect of acute heating on enhancing the activity of antioxidant enzymes, including superoxide dismutase (SOD), catalase (CAT), and glutathione peroxidase (GSH-Px). HSP25 shields skeletal muscle cells against damage caused by hydrogen peroxide, maybe by a process mediated by glutathione.[53] In addition to potentially reducing exercise-induced muscle damage, this heat-induced increase in antioxidant activity may also aid to reduce skeletal

muscle injury during human exercise training when combined with localized heat therapy employing microwave diathermy.

The RNA expression levels of COX-2 and IL-1β in the damaged gastrocnemius muscle tissues of SD rats by QT-PCR assay showed that microwave and BBR/Gel had a certain therapeutic effect on soft group injuries and the best effect was achieved by the combination of them, but the difference in therapeutic effect between the two treatment modalities was not obvious. The expression levels of IL-1β and COX-2 in the serum of SD rats were assessed using the enzyme-linked immunosorbent assay on days 1, 4, and 7. The results showed that: on the first day of treatment, the BBR/Gel and Mi +BBR/Gel groups demonstrated a significant inhibitory effect on both inflammatory factors because BBR was present. This could be explained by the mild aggravation of inflammation caused by the thermal effect of microwaves, or it could be the same as that in the NC group, suggesting that the microwaves had no therapeutic effect and even made the inflammation worse. Results from the fourth day of treatment indicated that the rats' serum IL-1β factor was not clearly inhibited by the Mi group, but the PGE2 factor in the rats' serum showed a sharp fall that was much lower than that of the BBR/Gel group.The two inflammatory factors in the rats' serum were inhibited by the BBR/Gel group, and their rate of drop was higher in this group than in the Model group. Additionally, the BBR/Gel group's influence on the natural recovery process was greater than that of the Model group. The two inflammatory variables dropped most quickly in the Mi+BBR/Gel group, and this group also saw the best therapeutic outcome. The BBR/Gel group had the second-best therapeutic impact, whereas the Mi group and the Mi +BBR/Gel group had similar therapeutic effects on the seventh day following therapy.

Throughout the whole process of inflammation dissipation, the BBR/Gel group has a stable therapeutic effect, which can stably inhibit the release of both inflammatory factors, while the Mi group has been inconspicuous or even has a slight increasing trend on inflammation in the early stage (1d), but the inhibition of inflammation is obvious in the middle stage (4d) and the late stage (7d), and there is a precipitous decrease of inflammatory factors, and the final result is superior to that of the BBR/Gel group, which is a process that shows that microwave therapy. The Mi+BBR/Gel group combined the advantages of the above two treatment modalities not only accelerated the process of tissue repair but also made the whole process more rapid and stable.

The results of the Western Blotting experiment showed that the three treatment groups had inhibitory effects on the expression of inflammatory factors COX-2 and IL-1β in the gastrocnemius muscle of SD rats with soft tissue injury. More specifically, the Mi group had an inhibitory effect on the inflammatory factor IL-1β that was stronger than that of the BBR/Gel group, and the Mi+BBR/Gel group had the strongest inhibitory effect, which was consistent with the expectations of the experiment. However, the BBR/Gel group's inhibitory effect was greater than that of the Mi group, the Mi+BBR/Gel group's inhibitory effect was stronger than the inhibitory effect of Mi group, and the BBR/Gel group's inhibitory effect was greater than that of the Mi group. There was no statistically significant difference in the inhibitory impact of the inflammatory factor COX-2 between the Mi+BBR/Gel group and the GB group, although the BBR/Gel group's effect was larger than the Mi group's.The reason for this outcome could be that, in the BBR/GelMA treatment mode, BBR penetrates deep into the gastrocnemius muscle tissue of rats through the skin and has a more evident inhibitory effect on COX-2 through the NF-κB pathway, whereas the inhibitory effect of microwaves on this factor is not as strong as that of BBR.

Considerable progress has been made with GelMA, but there are still several areas that need attention when translating it to the clinic. Future clinical applications are now focused on combinations of various cell types and different microencapsulation techniques working in a complementary mode. In addition, chemotherapy, gene and photothermal therapies combined with GelMA implantation can maximize therapeutic efficacy.[20] In recent years, domestic and foreign discussions on GelMA-based composite hydrogel scaffolds as a multifunctional platform for repairing severe bone defects have broken the limitations of external use of gels. On the other hand, the GelMA-based composite hydrogel serves as a filler for periosteal regeneration, promoting the process of bone repair.[54,55]

In treating skeletal muscle injury, the new BBR/Gel biogel has some therapeutic effects; however, these differ slightly from those of the 915HMz microwave. The experiment also opens up new avenues for the clinical application of BBR, and the introduction and use of gel will provide new insights into the treatment of topical cures for skeletal muscle injury. On the other hand, this experiment opens up the precedent of the comparison between physical factor therapy and topical gel therapy, which opens up new horizons for future topical drug experiments.

Conclusion

In this paper, we present the therapeutic effect of a BBR-loaded GelMA gel in combination with microwave therapy on skeletal muscle injury, and explore the mechanism of action and inflammation reduction in skeletal muscle repair during its treatment. Our experiments confirmed that BBR-loaded GelMA gel under microwave irradiation could alleviate muscle injury by down-regulating IL-1β, Cox-2 and PGE 2 factors in skeletal muscle, while promoting the repair process of muscle injury and shortening the disease development cycle. Microwave therapy combined with BBR/GelMA can effectively alleviate and treat skeletal muscle injuries and can be directly applied to the skin surface, which opens up the research direction of nano-biogel for the clinical treatment of skeletal muscle injuries. In the future, we will seek to develop a more effective composite nano-bio-gel by adding different clinically used drugs for the topical treatment of different diseases.

Acknowledgments

Would like to express our heartfelt gratitude to Zhao Duoyi from the Department of Orthopedics at the Fourth Hospital of China Medical University for his invaluable guidance throughout our experiments and his assistance in preparing this manuscript. We also wish to thank Professor Zhang Zhiyu for offering the collaborative opportunity that greatly enhanced the quality of our research. Additionally, we acknowledge the support from the Animal Experimentation Department and the Central Laboratory of the Fourth Hospital of China Medical University for providing the necessary experimental facilities. Tianhao Du and Liangliang Zhou and Jia Liu are regarded as co-first authors.

Funding

This work was supported by the Liaoning Provincial Science and Technology Program (Project No. 2022JH2/101500031).

Disclosure

The author(s) report no conflicts of interest in this work.

References

1. Rubio-Arias JÁ, Ávila-Gandía V, López-Román FJ, Soto-Méndez F, Alcaraz PE, Ramos-Campo DJ. Muscle damage and inflammation biomarkers after two ultra-endurance mountain races of different distances: 54 km vs 111 km. *Physiol Behav*. 2019;205:51–57. doi:10.1016/j.physbeh.2018.10.002
2. Rose C, Edwards K, Siegler J, Graham K, Caillaud C. Whole-body cryotherapy as a recovery technique after exercise: a review of the literature. *Int J Sports Med*. 2017;38(14):1049–1060. doi:10.1055/s-0043-114861
3. Safiri S, Kolahi A, Cross M, et al. Prevalence, deaths, and disability-adjusted life years due to musculoskeletal disorders for 195 countries and territories 1990–2017. *Arthritis Rheumatol*. 2021;73(4):702–714. doi:10.1002/art.41571
4. Gómez-Galán M, Pérez-Alonso J, Callejón-Ferre ÁJ, López-Martínez J. Musculoskeletal disorders: OWAS review. *Indust Health*. 2017;55(4):314–337. doi:10.2486/indhealth.2016-0191
5. Cento AS, Leigheb M, Caretti G, Penna F. Exercise and exercise mimetics for the treatment of musculoskeletal disorders. *Curr Osteoporos Rep*. 2022;20(5):249–259. doi:10.1007/s11914-022-00739-6
6. Chen GY, Nuñez G. Sterile inflammation: sensing and reacting to damage. *Nat Rev Immunol*. 2010;10(12):826–837. doi:10.1038/nri2873
7. Eltzschig HK, Eckle T. Ischemia and reperfusion—from mechanism to translation. *Nat Med*. 2011;17(11):1391–1401. doi:10.1038/nm.2507
8. Tu H, Li YL. Inflammation balance in skeletal muscle damage and repair. *Front Immunol*. 2023;14:1133355. doi:10.3389/fimmu.2023.1133355
9. Souza JD, Gottfried C. Muscle injury: review of experimental models. *J Electromyogr Kinesiol*. 2013;23(6):1253–1260. doi:10.1016/j.jelekin.2013.07.009
10. Brooks SV. Current topics for teaching skeletal muscle physiology. *Adv Physiol Educ*. 2003;27(4):171–182. doi:10.1152/advan.2003.27.4.171
11. Järvinen TAH, Järvinen TLN, Kääriäinen M, et al. Muscle injuries: optimising recovery. *Best Pract Res*. 2007;21(2):317–331. doi:10.1016/j.berh.2006.12.004
12. Zhou Y, Liu S, Ming J, Li Y, Deng M, He B. Sustained release effects of berberine-loaded chitosan microspheres on in vitro chondrocyte culture. *Drug Dev Ind Pharm*. 2017;43(10):1703–1714. doi:10.1080/03639045.2017.1339076
13. Wen CJ, Yu Y, Zong SY, et al. Berberine ameliorates collagen-induced arthritis in mice by restoring macrophage polarization via AMPK/mTORC1 pathway switching glycolytic reprogramming. *Int Immunopharmacol*. 2023;124:111024. doi:10.1016/j.intimp.2023.111024
14. Xia S, Jing R, Shi M, et al. BBR affects macrophage polarization via inhibition of NF-KB pathway to protect against T2DM-associated periodontitis. *J Periodont Res*. 2024;59(4):728–737. doi:10.1111/jre.13246
15. Vanti G, Coronnello M, Bani D, Mannini A, Bergonzi MC, Bilia AR. Co-delivery of berberine chloride and tariquidar in nanoliposomes enhanced intracellular berberine chloride in a doxorubicin-resistant K562 cell line due to P-gp overexpression. *Pharmaceutics*. 2021;13(3):306. doi:10.3390/pharmaceutics13030306

16. Song D, Hao J, Fan D. Biological properties and clinical applications of berberine. *Front Med*. 2020;14(5):564–582. doi:10.1007/s11684-019-0724-6
17. Li S, Sun J, Yang J, et al. Gelatin methacryloyl (GelMA) loaded with concentrated hypoxic pretreated adipose-derived mesenchymal stem cells (ADSCs) conditioned medium promotes wound healing and vascular regeneration in aged skin. *Biomater Res*. 2023;27(1):11. doi:10.1186/s40824-023-00352-3
18. Yue K, Trujillo-de Santiago G, Alvarez MM, Tamayol A, Annabi N, Khademhosseini A. Synthesis, properties, and biomedical applications of gelatin methacryloyl (GelMA) hydrogels. *Biomaterials*. 2015;73:254–271. doi:10.1016/j.biomaterials.2015.08.045
19. Jiang G, Li S, Yu K, et al. A 3D-printed PRP-GelMA hydrogel promotes osteochondral regeneration through M2 macrophage polarization in a rabbit model. *Acta Biomater*. 2021;128:150–162. doi:10.1016/j.actbio.2021.04.010
20. Lv B, Lu L, Hu L, et al. Recent advances in GelMA hydrogel transplantation for musculoskeletal disorders and related disease treatment. *Theranostics*. 2023;13(6):2015–2039. doi:10.7150/thno.80615
21. Rehman SRU, Augustine R, Zahid AA, Ahmed R, Tariq M, Hasan A. Reduced graphene oxide incorporated GelMA hydrogel promotes angiogenesis for wound healing applications. *IJN*. 2019;14:9603–9617. doi:10.2147/IJN.S218120
22. Gao Y, Wang Y, Duan Y, et al. 915MHz microwave ablation with high output power in in vivo porcine spleens. *Eur J Radiol*. 2010;75(1):87–90. doi:10.1016/j.ejrad.2009.03.009
23. Cheng Z, Xiao Q, Wang Y, Sun Y, Lu T, Liang P. 915MHz microwave ablation with implanted internal cooled-shaft antenna: initial experimental study in in vivo porcine livers. *Eur J Radiol*. 2011;79(1):131–135. doi:10.1016/j.ejrad.2009.12.013
24. Fu K, Lv X, Li W, et al. Berberine hydrochloride attenuates lipopolysaccharide-induced endometritis in mice by suppressing activation of NF-κB signal pathway. *Int Immunopharmacol*. 2015;24(1):128–132. doi:10.1016/j.intimp.2014.11.002
25. Zhao Y, Tian X, Liu G, Wang K, Xie Y, Qiu Y. Berberine protects myocardial cells against anoxia-reoxygenation injury via p38 MAPK-mediated NF-κB signaling pathways. *Exp Ther Med*. 2018. doi:10.3892/etm.2018.6949
26. rong ZJ, dan LH, Guo C, et al. Berberine attenuates ischemia–reperfusion injury through inhibiting HMGB1 release and NF-κB nuclear translocation. *Acta Pharmacol Sin*. 2018;39(11):1706–1715. doi:10.1038/s41401-018-0160-1
27. Jiang Q, Liu P, Wu X, et al. Berberine attenuates lipopolysaccharide-induced extracelluar matrix accumulation and inflammation in rat mesangial cells: involvement of NF-κB signaling pathway. *mol Cell Endocrinol*. 2011;331(1):34–40. doi:10.1016/j.mce.2010.07.023
28. Lai YF, Wang HY, Peng RY. Establishment of injury models in studies of biological effects induced by microwave radiation. *Military Med Res*. 2021;8(1):12. doi:10.1186/s40779-021-00303-w
29. Ge H, Wang Z, Yang Z, et al. Exploring the optimal impact force for chronic skeletal muscle injury induced by drop-mass technique in rats. *Front Physiol*. 2023;14:1241187. doi:10.3389/fphys.2023.1241187
30. Chen G, Huang Y, Huang C, et al. Decompression sickness-induced skeletal muscle injury: an animal model and pathological analysis. *Front Vet Sci*. 2024;11:1431110. doi:10.3389/fvets.2024.1431110
31. Farrell SG, Hatem M, Bharam S. Acute adductor muscle injury: a systematic review on diagnostic imaging, treatment, and prevention. *Am J Sports Med*. 2023;51(13):3591–3603. doi:10.1177/03635465221140923
32. Liu J, Liao Z, Wang J, et al. Research on skeletal muscle impact injury using a new rat model from a bioimpact machine. *Front Bioeng Biotechnol*. 2022;10:1055668. doi:10.3389/fbioe.2022.1055668
33. Bayer ML, Magnusson SP, Kjaer M. Early versus delayed rehabilitation after acute muscle injury. *N Engl J Med*. 2017;377(13):1300–1301. doi:10.1056/NEJMc1708134
34. Chen L, Fan XD, Qu H, Bai RN, Shi DZ. Berberine protects against TNF-α-induced injury of human umbilical vein endothelial cells via the AMPK/NF-κB/YY1 signaling pathway. Yong YK, ed. *Evidence-Based Complementary and Alternative Medicine*. 2021;2021:1–13. doi:10.1155/2021/6518355
35. El Assar M, Álvarez-Bustos A, Sosa P, Angulo J, Rodríguez-Mañas L. Effect of physical activity/exercise on oxidative stress and inflammation in muscle and vascular aging. *IJMS*. 2022;23(15):8713. doi:10.3390/ijms23158713
36. Yang W, Hu P. Skeletal muscle regeneration is modulated by inflammation. *J Orthop Transl*. 2018;13:25–32. doi:10.1016/j.jot.2018.01.002
37. Tsuchiya Y, Kitajima Y, Masumoto H, Ono Y. Damaged myofiber-derived metabolic enzymes act as activators of muscle satellite cells. *Stem Cell Report*. 2020;15(4):926–940. doi:10.1016/j.stemcr.2020.08.002
38. Dumont NA, Bentzinger CF, Sincennes M, Rudnicki MA. Satellite cells and skeletal muscle regeneration. In: Terjung R, editor. *Comprehensive Physiology*. 1st ed. Wiley; 2015:1027–1059. doi:10.1002/cphy.c140068
39. Schilling JD. Macrophages fuel skeletal muscle regeneration. *Immunometabolism*. 2021;3(2). doi:10.20900/immunometab20210013
40. Panci G, Chazaud B. Inflammation during post-injury skeletal muscle regeneration. *Semin Cell Dev Biol*. 2021;119:32–38. doi:10.1016/j.semcdb.2021.05.031
41. Al-Zaeed N, Budai Z, Szondy Z, Sarang Z. TAM kinase signaling is indispensable for proper skeletal muscle regeneration in mice. *Cell Death Dis*. 2021;12(6):611. doi:10.1038/s41419-021-03892-5
42. Feng Y, Cui Y, Gao JL, et al. Resveratrol attenuates neuronal autophagy and inflammatory injury by inhibiting the TLR4/NF-κB signaling pathway in experimental traumatic brain injury. *IntJ Mol Med*. 2016;37(4):921–930. doi:10.3892/ijmm.2016.2495
43. Wang C, Liu C, Liang C, et al. Role of berberine thermosensitive hydrogel in periodontitis via PI3K/AKT pathway in vitro. *IJMS*. 2023;24(7):6364. doi:10.3390/ijms24076364
44. Vardiman JP, Moodie N, Siedlik JA, Kudrna RA, Graham Z, Gallagher P. Short-wave diathermy pretreatment and inflammatory myokine response after high-intensity eccentric exercise. *Journal of Athletic Training*. 2015;50(6):612–620. doi:10.4085/1062-6050-50.1.12
45. Huard J, Li Y, Fu FH. Muscle injuries and repair: current trends in research. *J Bone Joint Surg Am*. 2002;84(5):822–832. doi:10.2106/00004623-200205000-00022
46. Giombini A, Giovannini V, Cesare AD, et al. Hyperthermia induced by microwave diathermy in the management of muscle and tendon injuries. *Br Med Bul*. 2007;83(1):379–396. doi:10.1093/bmb/ldm020
47. Shibaguchi T, Sugiura T, Fujitsu T, et al. Effects of icing or heat stress on the induction of fibrosis and/or regeneration of injured rat soleus muscle. *J Physiol Sci*. 2016;66(4):345–357. doi:10.1007/s12576-015-0433-0
48. Ament W, Verkerke GJ. Exercise and fatigue. *Sports Med*. 2009;39(5):389–422. doi:10.2165/00007256-200939050-00005
49. Mikami T, Yamauchi H. Preconditioning with whole-body or regional hyperthermia attenuates exercise-induced muscle damage in rodents. *Physiol Res*. 2022;125–134. doi:10.33549/physiolres.934569

50. Chen H, Adam A, Cheng Y, Tang S, Hartung J, Bao E. Localization and expression of heat shock protein 70 with rat myocardial cell damage induced by heat stress in vitro and in vivo. *Mol Med Rep*. 2015;11(3):2276–2284. doi:10.3892/mmr.2014.2986
51. Ogura Y, Naito H, Tsurukawa T, et al. Microwave hyperthermia treatment increases heat shock proteins in human skeletal muscle. *Br J Sports Med*. 2007;41(7):453–455. doi:10.1136/bjsm.2006.032938
52. Frier BC, Locke M. Heat stress inhibits skeletal muscle hypertrophy. *Cell Stress Chaper*. 2007;12(2):132. doi:10.1379/CSC-233R.1
53. Escobedo J, Pucci AM, Koh TJ. HSP25 protects skeletal muscle cells against oxidative stress. *Free Radic Biol Med*. 2004;37(9):1455–1462. doi:10.1016/j.freeradbiomed.2004.07.024
54. Zhang W, Wang N, Yang M, et al. Periosteum and development of the tissue-engineered periosteum for guided bone regeneration. *J Orthop Transl*. 2022;33:41–54. doi:10.1016/j.jot.2022.01.002
55. Xin T, Mao J, Liu L, et al. Programmed sustained release of recombinant human bone morphogenetic protein-2 and inorganic ion composite hydrogel as artificial periosteum. *ACS Appl Mater Interfaces*. 2020;12(6):6840–6851. doi:10.1021/acsami.9b18496